Charge-transfer Activation of Aromatic EDA Complexes with *N*-Nitrosopyridinium. Direct Comparison with the *N*-Nitropyridinium Acceptor

K. Y. Lee and J. K. Kochi*
Department of Chemistry, University of Houston, Houston, Texas 77204-5641, USA

The *N*-nitrosopyridinium cation ($PyNO^+$) forms a series of intermolecular EDA complexes with aromatic hydrocarbons which show distinctive charge-transfer absorption bands in the visible region. Upon standing at room temperature, the EDA complexes in acetonitrile undergo a redox transformation into nitric oxide and oxidative pyridine adducts at the *ipso* positions of such electron-rich donors as 1,4-dimethylnaphthalene and durene—the latter of which has been structurally characterized by X-ray crystallography. Since the same adducts are formed when the EDA complexes (at low temperatures) are deliberately irradiated at their charge-transfer absorption bands, an electron-transfer mechanism is readily delineated for both the thermal and photochemical activation of the aromatic EDA complexes with $PyNO^+$.

The nitronium ion (NO_2^+) and the nitrosonium ion (NO^+) are the most active electrophiles for effecting the nitration and nitrosation, respectively, of different aromatic substrates.[1,2] As coordinatively unsaturated cations, NO_2^+ and NO^+ are subject to ready anation to form neutral adducts (such as nitryl chloride and nitrosyl chlorides from chloride salts),[3] and they are both rapidly neutralized by nitrogen bases to form charged adducts (such as *N*-nitropyridinium and *N*-nitrosopyridinium from pyridine).[4,5] The latter are particularly interesting reagents since they can be effective in non-acidic (neutral) media,[6] and their electrophilic properties are subject to direct control by the judicious placement of various substituents on the heteroaromatic ring to modulate the pyridine base (donor) strength.[7] Indeed, we recently showed how a series of ring-substituted *N*-nitropyridinium salts can be exploited in the electrophilic (thermal) and charge-transfer (photochemical) nitration of different aromatic substrates (ArH),[8,9] eqn. (1).

$$ArH + PyNO_2^+ \xrightarrow{\Delta \text{ or } h\nu_{CT}} ArNO_2 + PyH^+ \quad (1)$$

Especially pertinent is the preequilibrium formation of an electron donor acceptor (EDA) complex, eqn. (2), that plays a

$$ArH + PyNO_2^+ \overset{K_{EDA}}{\rightleftharpoons} [ArH, PyNO_2^+] \quad (2)$$

seminal role in both the thermal and photochemical activation of aromatic nitration.[10] We now turn our attention to *N*-nitrosopyridinium as an analogous electrophilic reagent ($PyNO^+$)—especially since aromatic nitrosation is generally restricted to only the most reactive (electron-rich) donors such as phenols and anilines,[11] and it commonly occurs with a sizeable (proton) kinetic isotope effect.[12] Thus the latter suggests that the presence of the pyridine moiety in $PyNO^+$ could facilitate aromatic nitrosation by expeditious proton removal in a manner analogous to that in eqn. (1),[8,9] *i.e.*, eqn. (3).

$$ArH + PyNO^+ \xrightarrow{\Delta \text{ or } h\nu_{CT}} ArNO + PyH^+ \quad (3)$$

Since the electrophilic behaviour of *N*-nitrosopyridinium is largely unexplored, our studies initially focus on the charge-transfer (pre)equilibria with various aromatic donors [*cf.* eqn. (2)]. Most noteworthy, however, is our description of the unusual course of the electrophilic (thermal) and charge-transfer (photochemical) activation of $PyNO^+$ by the aromatic donors.

Results

N-Nitrosopyridinium hexachloroantimonate was prepared as light yellow crystals from the simple nitrosonium salts (NO^+-$SbCl_6^-$) by a procedure similar to that employed by Olah and co-workers for the tetrafluoroborate salt.[5] The diagnostic N–O stretching bands at ν_{NO} = 1814 cm^{-1} in the infrared spectrum of $PyNO^+$ $SbCl_6^-$ in Nujol mull and the characteristic ^1H NMR resonances at δ 8.09, 8.62 and 9.00 in CD_3CN solution were comparable to those originally reported for $PyNO^+$ BF_4^- in Nujol–Fluorolube mixed mull and liquid sulfur dioxide, respectively. The pale yellow solution of $PyNO^+$ $SbCl_6^-$ in acetonitrile remained unchanged at −40 °C, but the cation slowly decomposed with liberation of nitric oxide upon standing in the dark at room temperature (probably due to traces of moisture that were difficult to avoid in this hygroscopic solvent).

I. Charge-transfer Spectra of Aromatic EDA Complexes with the N-*Nitrosopyridinium Acceptor.*—Upon the addition of 1,4-dimethylnaphthalene (DMN) to the pale yellow $PyNO^+$ $SbCl_6^-$ dissolved in acetonitrile at −40 °C, the solution immediately took on a dark red-brown colouration, which was apparent in the UV–VIS spectrum as a broad low-energy tail on the local band of $PyNO^+$ in Fig. 1. Incremental additions of 1,4-dimethylnaphthalene and the spectral subtraction (shown in the inset) brought out the new absorption band with a constant λ_{max} of 460 nm.

Other relatively electron-rich aromatic donors such as durene (DUR), pentamethylbenzene (PMB), and hexamethylbenzene (HMB) also yielded coloured solutions when exposed to $PyNO^+$. Such colour changes were apparent in the electronic spectra by the appearance of an incomplete or partially resolved band (see Fig. 2), in which the low-energy absorption edge underwent a progressive red shift with increasing strengths of the aromatic (benzenoid) donors in the order: HMB > PMB > DUR. Since the new absorptions were not completely resolved, an alternative measure of the bathochromic shift is evaluated in Table 1 as $\lambda_{0.2}$, which was originally suggested by Tsubomura and Mulliken[13] for the quantification of charge-transfer absorption bands arising from structurally related donors.

The spectral behaviour of $PyNO^+$ with various aromatic

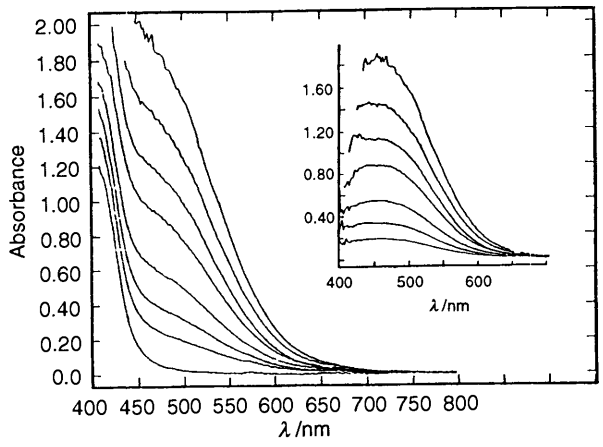

Fig. 1 Charge-transfer spectra obtained from 0.02 mol dm^{-3} $PyNO^+$ $SbCl_6^-$ and (top-to-bottom) 0.30, 0.20, 0.15, 0.10, 0.06, 0.04, 0.02 and 0 mmol dm^{-3} 1,4-dimethylnaphthalene in acetonitrile at −40 °C. Inset: difference spectra obtained from the (digital) subtraction of the $PyNO^+$ spectrum.

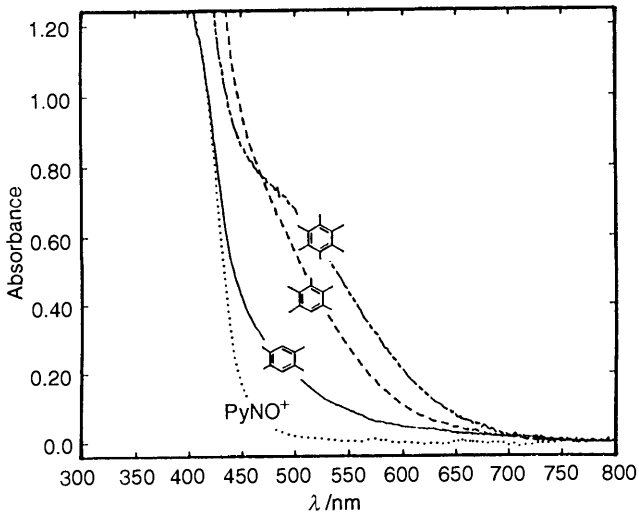

Fig. 2 Effect of aromatic donors (as indicated) on the low-energy absorptions of the *N*-nitrosopyridinium EDA complexes in acetonitrile solutions at −40 °C

donors bears a strong resemblance to the trend previously observed with the related *N*-nitropyridinium acceptors.[8] Accordingly, the spectral changes in Fig. 2 are assigned to the formation of analogous *N*-nitrospyridinium EDA complexes, eqn. (4).

$$ArH + PyNO^+ \overset{K_{EDA}}{\rightleftharpoons} [ArH, PyNO^+] \quad (4)$$

II. Formation Constant of the Aromatic EDA Complex with N-*Nitrosopyridinium Acceptor.*—The thermodynamic stability of the *N*-nitrosopyridinium EDA complex was evaluated by the Benesi–Hildebrand procedure,[14,15] *viz.* eqn. (5), where the CT

$$\frac{[ArH]}{A_{CT}} = \frac{1}{\varepsilon_{CT}} + \frac{1}{K_{EDA}\,\varepsilon_{CT}\,[PyNO^+]} \quad (5)$$

absorbance A_{CT} was measured with the aromatic donor added (incrementally in excess) to $PyNO^+$ in acetonitrile solution. 1,4-Dimethylnaphthalene (DMN) was the aromatic donor of choice for this measurement owing to its distinctive (*i.e.*, resolved) CT absorbance (Fig. 1). Values of the formation constant K_{EDA} [eqn. (4)] and the extinction coefficient ε_{CT} for

Table 1 Charge-transfer spectra of aromatic EDA complexes with the *N*-nitrosopyridinium acceptor[a]

Aromatic donor	E_i/eV	$\lambda_{0.2}$/nm[b]
Durene	8.05	498
Pentamethylbenzene	7.92	566
Hexamethylbenzene	7.85	600
1,4-Dimethylnaphthalene	7.78	460[c]

[a] In solution of 30 mmol dm^{-3} ArH and 30 mmol $PyNO^+$ $SbCl_6^-$ in acetonitrile at −40 °C. [b] Wavelength at which absorbance is 0.2 (see the text), except as indicated otherwise. [c] λ_{max}.

Table 2 Formation constant of the EDA complex of 1,4-dimethylnaphthalene and *N*-nitrospyridinium cation[a]

λ_{mon}/nm[b]	K_{EDA}/dm^3 mol^{-1}	ε_{CT}/dm^3 mol^{-1} cm^{-1}	r[c]
460	2.21	230	0.997
480	2.15	225	0.998
500	2.15	203	0.998
520	2.32	156	0.998
540	2.87	99	0.997
	2.2 ± 0.1[d]	200 ± 30[d]	

[a] In solutions containing 0.02 mol dm^{-3} $PyNO^+$ $SbCl_6^-$ and 0.02–0.3 mol dm^{-3} 1,4-dimethylnaphthalene in acetonitrile at −40 °C. [b] Monitoring wavelength. [c] Correlation coefficient. [d] Average of first four determinations.

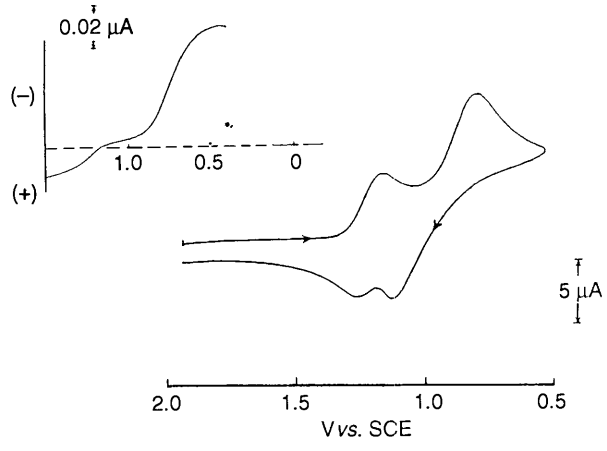

Fig. 3 Initial negative-scan cyclic voltammogram of 5 mmol dm^{-3} $PyNO^+$ $SbCl_6^-$ in acetonitrile containing 0.1 mol dm^{-3} TBAH at v = 0.5 V s^{-1}. Inset: steady-state voltammogram of $PyNO^+$ $SbCl_6^-$ at a platinum ultramicroelectrode (as above).

[DMN, $PyNO^+$] were measured at various monitoring wavelengths (see the resolved low-energy tail in Fig. 1, inset) and are listed in Table 2. We conclude from the limited magnitude of K_{EDA} = 2.3 dm^3 mol^{-1} that the *N*-nitrosopyridinium EDA complex (like its *N*-nitropyridinium analogue)[8] is to be considered weak according to Mulliken's criterion.[16]

III. Reduction Potential of the N-*Nitrosopyridinium Acceptor.*—The electron-acceptor properties of the *N*-nitrosopyridinium acceptor were evaluated by cyclic voltammetry of $PyNO^+$ $SbCl_6^-$ at a platinum electrode in acetonitrile solution containing 0.1 mol dm^{-3} tetra-*n*-butylammonium hexafluoroantimonate (TBAH) as the supporting electrolyte. The initial negative-scan cyclic voltammogram at the scan rate v = 0.5 V s^{-1} (Fig. 3) showed two well-defined cathodic peaks, a minor one at C_1 = 1.23 V, and a major one at C_2 = 0.80 V *vs.* SCE. On the return scan, a pair of anodic peaks appeared at A_2 = 1.20 V and A_1 = 1.33 V. When the initial negative scan was switched at E_{sw} = 1.0 V, immediately following C_1, only the anodic peak at A_1 = 1.33 V was observed. The redox couple

C_1/A_1 was thus readily assigned to the reversible NO^+/NO interchange based on the previous study.[17] On the other hand, sweep-rate dependence of the cyclic voltammogram showed that the second cathodic wave C_2 was chemically irreversible. Since the second wave A_2 was in fact coincident with the anodic behaviour of nitric oxide in the presence of pyridine, the cathodic process associated with C_2 was ascribed to eqn. (6).

$$PyNO^+ + e \xrightarrow{C_2} [PyNO^\bullet] \xrightarrow{fast} Py + NO^\bullet \quad (6)$$

Indeed, such a dissociative electron attachment was analogous to that previously observed in the reduction of the *N*-nitropyridinium acceptor.[8] Consequently, the anodic wave A_2 was assigned to the associative electron detachment in eqn. (7).

$$NO^\bullet - e \xrightarrow[Py]{[A_2]} PyNO^+ \quad (7)$$

Although the precise origin of NO^+ for the coupled C_1/A_1 wave is unknown (*vide supra*), it does not arise *via* the dissociation of *N*-nitrosopyridinium according to eqn. (8). This conclusion is

$$PyNO^+ \underset{CH_3CN}{\rightleftharpoons} Py + NO^+ \quad (8)$$

evident from the direct analysis for free NO^+ extant in acetonitrile solutions of *N*-nitrosopyridinium by steady-state voltammetry employing ultramicroelectrodes.[18] Thus the inset to Fig. 3 shows the steady-state voltammogram of $PyNO^+$ $SbCl_6^-$ dissolved in acetonitrile to contain nitric oxide, but essentially no NO^+. We tentatively conclude that the partial decomposition of $PyNO^+$ in (wet) acetonitrile was responsible for the liberation of NO,[19] which in turn was rapidly oxidized to NO^+ at the initial (positive) potential of the CV experiment.

IV. Dissociation of N-*Nitrosopyridinium in Acetonitrile.*—The extent to which the *N*-nitrosopyridinium acceptor suffers the (reversible) dissociation expressed in eqn. (8), was evaluated by two independent titrimetric procedures. In the first method, the competitive complexation of NO^+ with an aromatic donor durene (DUR) and the sterically hindered pyridine base 2,6-lutidine (Lu) was considered as

$$\frac{[DUR, NO^+]}{K_1[DUR]} = \frac{[Lu\,NO^+]}{K_2[Lu]} \quad (9)$$

where K_1 and K_2 refer to the associative equilibria given in eqns. (10) and (11) and the competition can be quantitatively

$$DUR + NO^+ \overset{K_1}{\rightleftharpoons} [DUR,NO^+] \quad (10)$$

$$Lu + NO^+ \overset{K_2}{\rightleftharpoons} LuNO^+ \quad (11)$$

examined by spectral titration. For example, Lu was added incrementally to the red-brown solution of the EDA complex prepared from DUR and NO^+ BF_4^- in acetonitrile, with λ_{CT} = 357 nm, ε_{CT} = 1100 dm^3 mol^{-1} cm^{-1}.[20a] Upon the addition of each Lu aliquot, the 357 nm absorbance decreased monotonically, but reached a limiting value at which the CT spectrum did not change upon further increasing the Lu concentration. Accordingly, from the value of K_1 = 450 dm^3 mol^{-1} determined in the earlier study,[20a] the association constant K_2 was roughly evaluated at the intermediate Lu concentrations as 3 ± 2 × 10^3 dm^3 mol^{-1}, as described in the Experimental section.

By an alternative but less precise titrimetric method, the concentration of free NO^+ in the presence of Lu was determined directly by steady-state voltammetry (*vide supra*). Thus the steady-state voltammogram of a 10 mmol dm^{-3} solution of NO^+ BF_4^- in acetonitrile containing 0.1 mol dm^{-3} TBAH showed $E_{\frac{1}{4}}$ = 1.28 V *vs.* SCE,[18] with traces of (adventitious) nitric oxide in evidence. When a small aliquot of Lu was added, the limiting current of NO^+ decreased and a new cathodic wave at 0.63 V *vs.* SCE was observed for the adduct $LuNO^+$ (compare Fig. 3). Upon further incremental additions of Lu, the cathodic current for $LuNO^+$ increased concomitantly with the decrease of the cathodic current of NO^+ until a limiting current was attained at 1.28 V. This established the concentration of free NO^+, and the association constant for K_2 was readily evaluated as *ca.* 5 × 10^2 dm^3 mol^{-1}, as described in the Experimental section. Although the magnitude of K_2 from the two methods was somewhat disparate (partially due to differences in the salt effect), the results were sufficient to conclude that the association of NO^+ with the pyridinium base was extensive, but not complete.

V. Thermal Activation of the N-*Nitrosopyridinium Acceptor by Aromatic Donors.*—The strongly coloured solutions of the aromatic EDA complexes with $PyNO^+$ decolourized when allowed to stand in the dark at room temperature, with the rate of bleaching qualitatively decreasing in the order: 1,4-dimethylnaphthalene (DMN) > hexamethylbenzene (HMB) > durene (DUR) ≫ *p*-xylene (XYL) > toluene (TOL). Since all of these colours persisted indefinitely when the solutions were merely cooled to −40 °C and protected from light (even adventitious roomlight), the chemical transformations accompanying the colour changes are (arbitrarily) designated hereafter as *thermal* (*electrophilic*) reactions as follows.

1,4-*Dimethylnaphthalene.* The dark red solution of the EDA complex made up from equimolar amounts of dimethylnaphthalene and $PyNO^+$ $SbCl_6^-$ at acetonitrile at −40 °C, upon warming to room temperature turned yellow within 30 min. Spectral (^{1}H NMR) examination revealed the complete disappearance of DMN (δ 7.21, 2.61) and its replacement by a new species with a characteristic vinyl resonance at δ 6.05 and a pair of methyl resonances at δ 2.44 and 2.25. Isolation of the organic products by removal of the solvent *in vacuo*, followed by fractional crystallization, afforded two isomeric adducts which were characterized as the *cis* and *trans* adducts **1a**, **b** in more or less equal amounts (see the Experimental section).

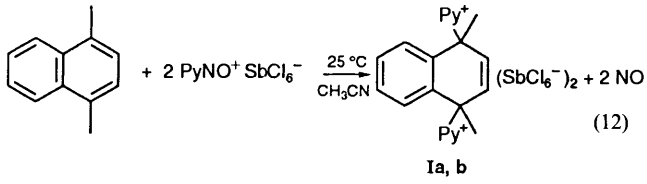

(12)

1a, b

The redox stoichiometry in eqn. (12) received support from the accompanying change in the IR spectrum, in which the N–O stretching band of the nitrosopyridinium EDA complex (ν_{NO} = 1857 cm^{-1}) was replaced by that of nitric oxide (ν_{NO} = 1876 cm^{-1}).[20b] The same transformation was observed (see Table 3) when *N*-nitrosopyridinium was generated *in situ* by the addition of pyridine to a solution of the EDA complex of dimethylnaphthalene and NO^+ BF_4^- at room temperature [compare eqns. (10) and (11)]. Control experiments established that DMN and NO^+ BF_4^- were essentially unchanged in the absence of pyridine, under otherwise the same conditions.

Durene. When the red-brown solution of the EDA complex of durene and $PyNO^+$ $SbCl_6^-$ was slowly stirred in the dark at room temperature, a yellow solid separated over the course of a day. The well-resolved ^{1}H NMR spectrum revealed the

Table 3 Thermal and charge-transfer activation of aromatic EDA complexes with the *N*-nitropyridinium acceptor[a]

Aromatic donor	(μmol)	$PyNO^+$ [b] (μmol)	Activation[c]	Adduct (μmol)	Rec.[d] (μmol)
1,4-Dimethylnaphthalene	(90)	$SbCl_6^-$ (150)	T (23 °C), 30 min	**Ia** (30), **Ib** (22)	28
	(30)	$SbCl_6^-$ (30)	P (> 520 nm), −40 °C, 5 h	**Ia** (4.5), **Ib** (3.5)	18
	(150)	BF_4^- (150)	T (23 °C), 1 h	**Ia** (16), **Ib** (12)	< 0.5
Durene	(90)	$SbCl_6^-$ (150)	P (> 500 nm), 0 °C, 8 h	**IIa** (35), **IIb** (O)	42
	(80)	$SbCl_6^-$ (190)	T (23 °C), 24 h	**IIa** (47), **IIb** (0)	25
	(75)	BF_4^- (150)	P (> 500 nm), 0 °C, 7 h	**IIa** (27), **IIb** (20)	24
	(75)	BF_4^- (150)	T (23 °C), 24 h	**IIa** (18), **IIb** (15)	40
	(30)	BF_4^- (150)	T (23 °C), 24 h	**IIa** (16), **IIb** (12)	< 0.5

[a] In 0.4 cm^3 CD_3CN. [b] As isolated $PyNO^+$ $SbCl_6^-$ salt or $PyNO^+$ BF_4^- prepared *in situ*. [c] T = thermal, P = charge-transfer, temp., duration. [d] Recovered ArH.

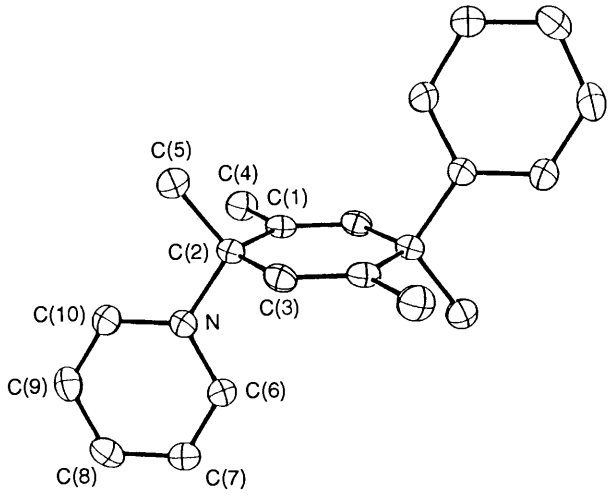

Fig. 4 ORTEP diagram of **IIa**, the oxidative bis-pyridine adduct to the *ipso* position of durene showing the *trans* stereochemistry

presence of the characteristic vinyl resonance δ 6.11 and a pair of methyl resonances at δ 1.61 and 2.17. Isolation of the organic product by the removal of acetonitrile *in vacuo* afforded a labile yellow solid which could not be successfully crystallized without decomposition (*vide infra*). Accordingly, a carefully prepared solution of durene and $PyNO^+$ $SbCl_6^-$ was allowed to stand quietly in the dark with no stirring. Single crystals suitable for X-ray crystallography were obtained after 3 days and washed with ice-cold acetonitrile under an argon atmosphere. The ORTEP diagram presented in Fig. 4 established the thermal product to be the 1,4-durene adduct **IIa** with *trans* stereochemistry, eqn. (13).

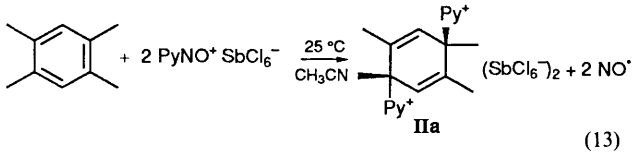

(13)

In contrast with the single isomer formed in eqn. (13), the decomposition of the durene EDA complex with the tetrafluoroborate salt $PyNO^+$ BF_4^- (prepared *in situ*) afforded a roughly equimolar mixture of the *trans* adduct **IIa** [eqn. (13)] and its *cis* isomer **IIb** (for details, see the Experimental section), *i.e.*, eqn. (14).

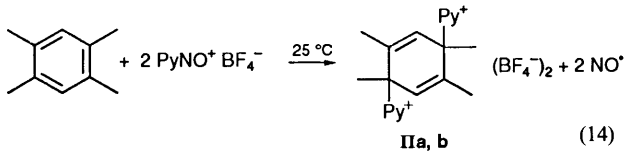

(14)

Solutions of the durene adduct **IIa** and/or **IIb** in acetonitrile slowly decomposed over the course of several days to afford a new salt **IIc**, the ^1H NMR spectrum of which showed a unique resonance at δ 5.66 that was assigned to *N*-(2,4,5-trimethylbenzyl)pyridinium cation in comparison with the chemical shift of the benzyl protons at δ 5.59 in an analogous lutidinium derivative,[21] eqn. (15).

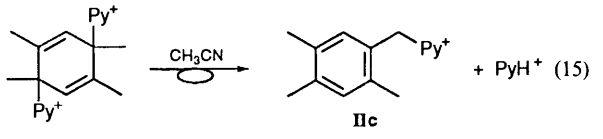

(15)

Hexamethylbenzene. The EDA complex of hexamethylbenzene and $PyNO^+$ BF_4^- (prepared *in situ*) was prepared in acetonitrile at −40 °C. As the brown solution was warmed to room temperature, transient methyl resonances at δ 1.40 and 1.49 were observed; these new resonances disappeared simultaneously with the (unchanged) HMB resonance (δ 2.18) over the course of a day. Since the final product was assigned to *N*-(pentamethylbenzyl)pyridinium cation (δ 5.89) by analogy with the *p*-cyanopyridinium analogue (δ 5.93) prepared independently, we inferred that the oxidative substitution of HMB proceeded *via* a rapid sequence of addition and elimination, *i.e.*, eqn. (16), in contrast with the behaviour of durene, in which the separate steps are temporally resolved [see eqns. (13) and (14)].

p-Xylene and toluene. The yellow (orange) solutions of the EDA complexes of either toluene or *p*-xylene and $PyNO^+$ BF_4^- (prepared *in situ*) were visually unchanged when allowed to stand at room temperature in the dark for several days; gas chromatographic analysis indicated the aromatic donors could be recovered intact. However, the coloured solutions were bleached when deliberately irradiated with visible light with λ_{exc} > 380 nm. Spectral (^1H NMR) examination of the

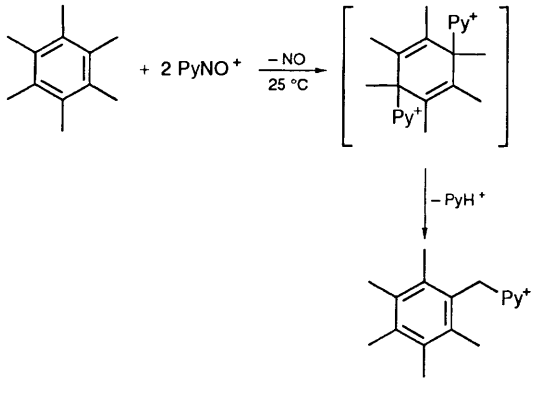

(16)

photolysate indicated that the amounts of toluene and *p*-xylene were greatly diminished, and their methyl resonances were replaced by multiple new resonances (see the Experimental section) indicative of mixtures of products which were not analysed further. Instead, we focussed our attention on the photoinduced transformation of the EDA complexes of dimethylnaphthalene and durene as a basis for the comparison with the thermal (electrophilic) processes described in the foregoing section.

VI. Photochemical Activation of Aromatic EDA Complexes with the N-*Nitrosopyridinium Acceptor.*—Owing to the thermal stability of the aromatic EDA complexes with $PyNO^+$ $SbCl_6^-$ at −40 °C, the coloured solutions were directly irradiated at this low temperature with filtered (visible) light selected to excite only the low-energy tails of the charge-transfer bands in Fig. 2. Accordingly, the chemical transformations accompanying such an irradiation resulted unequivocally from the specific *charge-transfer activation* of the aromatic EDA complexes in the following way.

1,4-*Dimethylnaphthalene.* The dark red solution of the EDA complex of dimethylnaphthalene and $PyNO^+$ $SbCl_6^-$ in acetonitrile at −40 °C was irradiated with the focussed output of a 500 W mercury lamp equipped with a sharp cut-off filter to allow the passage of light with $\lambda_{exc} > 540$ nm. Such an excitation radiation ensured that only the low-energy tail of the charge-transfer band of the [DMN, $PyNO^+$] complex was irradiated (compare Fig. 2). Continuous monitoring by ^1H NMR spectroscopy at −40 °C showed the characteristic resonances of DMN (δ 7.21, 2.61) to disappear gradually over the 5 h irradiation. Final analysis of the photolysate indicated that all the dimethylnaphthalene was consumed, and in its place was the mixture of bis-pyridine adducts **Ia** and **Ib** in essentially equimolar amounts, eqn. (17). The isomeric composition of the photochemical adducts in eqn. (17) was the same as that formed in the thermal process (see Table 3), as readily indicated from the comparative ^1H NMR spectra of the product mixtures.

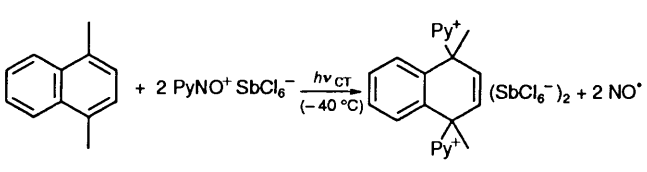

Ia, b (17)

Durene. Irradiation of the red-brown solution of the durene EDA complex with $PyNO^+$ $SbCl_6^-$ at 0 °C was carried out with the aid of Pyrex sharp cut-off filter for $\lambda_{exc} > 500$ nm (compare Fig. 2). Spectral (^1H NMR) analysis of the photolysate indicated the presence of a single isomeric adduct **IIa**, together with unchanged durene, eqn. (18).

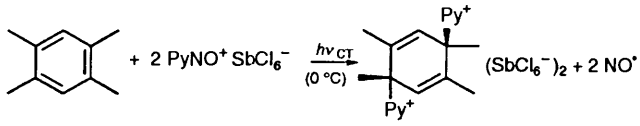

IIa (18)

The charge-transfer activation of the durene EDA complex prepared from $PyNO^+BF_4^-$ (generated *in situ*) was similarly carried out with $\lambda_{exc} > 500$ nm. Spectral (^1H NMR) analysis of the photolysate indicated that both isomeric adducts **IIa** and **IIb** were formed in roughly equimolar amounts, *i.e.*, eqn. (19).

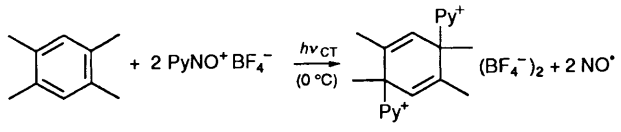

IIa, b (19)

On standing, both adducts were converted into the benzylic pyridinium salt **IIc** according to eqn. (15).

Discussion

The *N*-nitrosopyridinium ion $PyNO^+$ is a viable electron acceptor by virtue of the facile formation of intermolecular electron donor–acceptor (EDA) complexes with various aromatic hydrocarbons according to eqn. (4). As such, it bears a strong resemblance to *N*-nitropyridinium ion $PyNO_2^+$ examined in the previous study.[8,9] Indeed, the strengths of these cationic acceptors are both characterized by the relatively positive potentials at which they undergo cathodic reduction. Although the direct electrochemical comparison of the acceptor strengths of $PyNO^+$ and $PyNO_2^+$ is not quantitatively feasible, their related cyclic voltammetric behaviour[8] is sufficient to classify them as more or less comparable electron acceptors. Essentially the same conclusion is reached by a comparison of the charge-transfer spectra of aromatic EDA complexes with $PyNO^+$ in Fig. 2 relative to the corresponding spectra obtained with $PyNO_2^+$ in the earlier study.[8] Since the charge-transfer transition energies ($h\nu_{CT}$) of the nitropyridinium EDA complexes have been demonstrated by time-resolved (picosecond) spectroscopy to correspond to the electronic (vertical) transition within the EDA complex to the ion radical pair state,[9] *i.e.*, eqn. (20), we infer from the spectral similarities of the two

$$[ArH,PyNO_2^+] \xrightarrow{h\nu_{CT}} [ArH^{\bullet+},PyNO_2^{\bullet}] \quad (20)$$

series of aromatic EDA complexes that an analogous charge-transfer activation applies to the nitrosopyridinium complexes, *i.e.*, eqn. (21). On this basis, the small but consistent red shift in

$$[ArH,PyNO^+] \underset{k_{-1}}{\overset{h\nu_{CT}}{\rightleftharpoons}} [ArH^{\bullet+},PyNO^{\bullet}] \quad (21)$$

the CT spectra of aromatic EDA complexes with $PyNO^+$ relative to those of $PyNO_2^+$ indicates that *N*-nitrosopyridinium is even a somewhat better acceptor than the *N*-nitro analogue.[22]

Charge-transfer Activation of Aromatic EDA Complexes with N-*Nitrosopyridinium.*—The enhanced acceptor properties of $PyNO^+$ is manifested in its facile thermal reaction with aromatic donors, especially with the relatively electron-rich dimethylnaphthalene, hexamethylbenzene and durene, as described in eqns. (12)–(14) and (16). However, the complex stoichiometry associated with these redox transformations does not readily conform to the expected (electrophilic) behaviour of $PyNO^+$ simply to transfer a nitrosonium moiety according to eqn. (3).

In order to resolve this mechanistic problem, let us focus on the same transformations that are effected in eqns. (17)–(19) by the direct irradiation of the charge-transfer absorption band according to eqn. (21). Although the photoefficiency of the photoinduced electron transfer was not measured, the relatively short irradiation times required for complete reaction indicated that energy wastage in eqn. (21) by back electron transfer (k_{-1}) did not pose a serious complication. Indeed the labile character of the nitrosopyridinyl radical [indicated in eqn. (6) by cyclic voltammetric studies] is consistent with a fast fragmentation ($k_f > k_{-1}$) that effectively precludes back electron transfer[23] (Scheme 1).

$$[ArH,PyNO^+] \underset{k_{-1}}{\overset{h\nu_{CT}}{\rightleftharpoons}} [ArH^{\bullet+},PyNO^{\bullet}] \quad (21)$$

$$[ArH^{\bullet+},PyNO^{\bullet}] \xrightarrow{k_f} [ArH^{\bullet+},Py,NO^{\bullet}] \quad (22)$$

Scheme 1

The subsequent fate of the reactive triad in eqn. (22) can be deduced from the pyridine-derived *ipso* adducts **I** and **II** formed from dimethylnaphthalene and durene, respectively. Thus Parker and others have shown that aromatic cation radicals ($ArH^{\bullet+}$) are highly susceptible to nucleophilic addition, especially by pyridine bases,[24] Scheme 2.

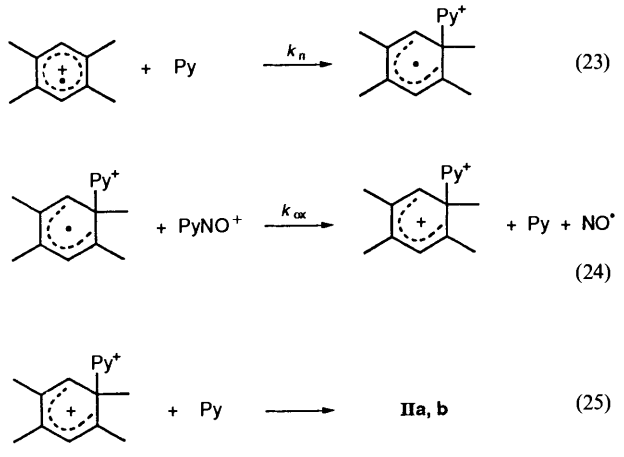

Scheme 2

According to Scheme 2, nucleophilic collapse (k_n) occurs in the durene cation radical at the *ipso* carbon which corresponds to the position of highest charge density.[25] The reduction potential of $PyNO^+$ [see eqn. (6)] is sufficient to oxidize rapidly the distonic cation radical adduct to the dication in eqn. (24).[26] The counter-ion plays a stereochemical role in the addition of the second pyridine [see eqn. (25), since only the *trans* adduct **IIa** is formed when $SbCl_6^-$ is employed in eqn. (13), whereas an equimolar mixture of *trans*/*cis* isomers (**IIa, b**) is produced from the BF_4^- salt in eqn. (14). However, the ionic effect is not observed with 1,4-dimethylnaphthalene [eqn. (12)], which affords essentially the same mixtures of *trans*/*cis* adducts (**Ia, b**), irrespective of whether $PyNO^+$ $SbCl_6^-$ or $PyNO^+$ BF_4^- is employed.

Since the stereoselectivity observed in the oxidative addition generally correlates with the size of the aromatic donor and the anionic counterion, we ascribe it to ion-pairing effects—the energetics of which are likely to be rather small in a polar solvent such as acetonitrile.[27] More importantly, such subtle stereochemical consequences provide a sensitive mechanistic probe for interpreting the comparative thermal and photochemical transformations of aromatic EDA complexes with nitrosopyridinium salts. Thus we conclude from the striking parallel in the stereochemical course of oxidative additions, as described in Table 3, that the sequential reactions of the reactive intermediates outlined in Scheme 2 are equally applicable to the *thermal* activation of aromatic EDA complexes. It is important to emphasize that the photochemical processes are carried out under the same conditions, but merely at low temperatures where the thermal reactions are too slow to compete. Accordingly, the charge-transfer activation of the aromatic EDA complex can alternatively be cast for the thermal process as Scheme 3.

$$ArH + PyNO^+ \overset{K_{EDA}}{\rightleftharpoons} [ArH,PyNO^+] \quad (26)$$

$$[ArH,PyNO^+] \xrightarrow{k_E} ArH^{\bullet+} + Py + NO^{\bullet} \quad (27)$$

Scheme 3

Since electron transfer (k_E) represents the adiabatic counterpart to the photochemical process ($h\nu_{CT}$), the triad in eqn. (27) is equivalent to that formed in Scheme 1.[27]

Comments on the Comparative CT Behaviour of N-*Nitrosopyridinium and* N-*Nitropyridinium Acceptors.*—Despite the similar redox properties of $PyNO^+$ and $PyNO_2^+$, and the related charge-transfer transitions in the two series of aromatic EDA complexes, this pair of acceptors ultimately leads to strongly differentiated products. Thus the oxidative adducts **IIa, b** obtained from durene with $PyNO^+$ bear little resemblance to the substituted nitrodurenes obtained with $PyNO_3^+$.[8,9] The difference in products must therefore be associated with the divergent pathways for the reactive triads, that is, $[ArH^{\bullet+},Py,NO_2^{\bullet}]$ and $[ArH^{\bullet+},Py,NO^{\bullet}]$, subsequent to the rate-limiting CT activations in eqns. (20) and (21), respectively. The former has been shown to lead to aromatic nitration primarily *via* the prior homolytic collapse (k_r) of the aromatic cation radical with $NO_2^{\bullet}$, followed by deprotonation (k_H), Scheme 4.

$$[ArH^{\bullet+},Py,NO_2^{\bullet}] \xrightarrow{k_r} \overset{+}{Ar}(H)(NO_2) + Py \quad (28)$$

$$\overset{+}{Ar}(H)(NO_2) + Py \xrightarrow{k_H} ArNO_2 + PyH^+ \quad (29)$$

Scheme 4

By analogy, the homolytic collapse of the aromatic cation radical with $NO^{\bullet}$ would result in aromatic nitrosation, Scheme 5.

$$[ArH^{\bullet+},Py,NO^{\bullet}] \overset{k_r}{\rightleftharpoons} \overset{+}{Ar}(H)(NO) + Py \quad (30)$$

$$Ar(H)(NO) + Py \xrightarrow{k_H} ArNO + PyH^+ \quad (31)$$

Scheme 5

However, the absence of nitrosoarenes among the products from $PyNO^+$ in Table 3 indicates that the collapse of the triad

according to Scheme 5 is not competitive with the nucleophilic collapse in Scheme 2. This conundrum is resolved if the homolytic collapse in eqn. (30) is readily reversible, and the deprotonation k_H in eqn. (31) is (relatively) slow. The latter is experimentally supported by the earlier observations of relatively large deuterium kinetic isotope effects (KIE) for aromatic nitrosation, which may be as large as $k_H/k_D = 4.5$.[28] By contrast, the deprotonation step is kinetically unimportant in aromatic nitration (only in unusual cases[29] is $k_H/k_D > 1$), and thus reversibility in the formation of the Wheland intermediate generally does not pose a serious kinetic complication. According to this formulation, aromatic nitrosation by $PyNO^+$ and aromatic nitration by $PyNO_2^+$ are distinguished by the rates of deprotonation of the Wheland intermediates [*i.e.*, $Ar(NO)H^+$ and $Ar(NO_2)H^+$] relative to their homolytic scission to regenerate $ArH^{\bullet+}$ and $NO^\bullet$ or $NO_2^\bullet$.[30] (Note that the nucleophilic addition to $ArH^{\bullet+}$ is common to both processes.) Interestingly, this mechanistic conclusion leads to the prediction that charge-transfer activation of aromatic nitrosation should be possible, provided there is no competition for $ArH^{\bullet+}$ from nucleophilic addition (*e.g.*, if only weakly nucleophilic or sterically encumbered bases were available in the reaction milieu).

Experimental

Materials.—Nitrosonium tetrafluoroborate (Strem) was recrystallized from a mixture of acetonitrile and dichloromethane at −40 °C. Nitrosonium hexachloroantimonate was prepared from nitrosyl chloride[31] and antimony pentachloride.[32] *N*-Nitrosopyridinium hexachloroantimonate was prepared by dissolving 3.2 g of NO^+ $SbCl_6^-$ in 60 cm^3 of acetonitrile followed by the slow addition at −20 °C of a solution containing 1 equivalent (0.71 cm^3) of pyridine in 20 cm^3 of acetonitrile. The yellow solution was stirred for 30 min at 0 °C and then evaporated *in vacuo*. The yellow crystals of $PyNO^+$ $SbCl_6^-$ were recrystallized from acetonitrile at −20 °C. IR: 1814 cm^{-1} (Nujol), and 1859 cm^{-1} (nitromethane). δ_H-(CD_3CN) 8.09 (t, 2 H), 8.62 (t, 1 H) and 9.00 (d, 2 H). All the aromatic donors employed in this study have been described previously.[8,23] Acetonitrile (Fisher reagent grade) was stirred with $KMnO_4$ for 24 h and the mixture refluxed until colourless. After removal of the brown MnO_2 by filtration, the acetonitrile was distilled from P_2O_5 under an argon atmosphere. Acetonitrile was again fractionated from CaH_2 and stored in a Schlenk flask under an argon atmosphere.

Instrumentation and Analysis.—The UV–VIS absorption spectra were measured on a Hewlett-Packard model 8450A diode-array spectrometer equipped with an HP 89100A temperature controller. The ^1H NMR spectra were recorded on a JEOL FX 90Q spectrometer operating at 89.55 MHz, and the proton chemical shifts are reported in ppm downfield from a tetramethylsilane internal standard. IR spectra were obtained on a Nicolet 10DX FT spectrometer with 4 cm^{-1} resolution. GC–MS analyses were carried out on a Hewlett-Packard 5890 chromatograph interfaced to an HP 5970 mass spectrometer (EI, 70 eV). High performance liquid chromatography (HPLC) employed an LDC Analytical model 3000 equipped with dual pumps (constaMetric 3200 and 3500 solvent delivery systems) and UV detector (spectroMonitor 3100). Analytical HPLC was carried out with a reversed-phase column (Hypersil BDS C_{18}, 5 μ). Electrochemical measurements were carried out as described earlier.[18]

The light source for charge-transfer nitration consisted of a 500 W (Osram HB) mercury lamp equipped with a parabolic reflector. The light beam was passed through a circulating water filter to remove IR radiation, and a fused silica biconvex lens ($\varphi = 4.5$ cm, $f = 10$ cm) focussed the light into the centre of a 1.0 cm quartz cuvette. A sharp cut-off filter (Corning CS-3 series) was fixed in front of the cell to ensure that only the charge-transfer band of the relevant EDA complex was irradiated. Temperature control was achieved by immersing the sample cuvette in a stirred acetone bath that was contained in Pyrex dewar and cooled automatically in the temperature range −60 to −40 ± 2 °C with the aid of a Neslab CC-65A immersion chiller.

Competitive Equilibria of Nitrosonium with 2,6-Lutidine and Durene by Spectral Methods.—An equimolar solution of durene (DUR, 6.7 mmol dm^{-3}) and NO^+ BF_4^- (6.7 mmol dm^{-3}) in acetonitrile shows $\lambda_{CT} = 357$ nm and a long low-energy tail in the visible region. Upon the incremental addition of 2,6-lutidine (Lu, 3.6 and 7.2 mmol dm^{-3}), the visible absorption decreased but reached a limit at 10.8 mmol dm^{-3} Lu and A_{CT} did not change at 14.4 mmol dm^{-3} Lu. Let $[DUR]_0 = [DUR] + [NO^+, DUR]$, $[NO]_0 = [NO^+] + [NO^+, DUR] + [LuNO^+]$ and $[Lu]_0 = [Lu] + [LuNO^+]$. From the equilibria in eqns. (10) and (11), it follows that $[NO^+] = [NO^+, DUR]/K_1([DUR]_0 - [NO^+,DUR])$,$[LuNO^+] = [NO^+]_0 - [NO^+] - [NO^+, DUR]$ and therefore, $K_2 = [LuNO^+] = [NO^+]([Lu]_0 - [LuNO^+])$. At the initial concentrations $[DUR]_0$, $[NO^+]_0$ and $[Lu]_0$ and the spectrally determined A_{CT} for $[NO^+, DUR]$, the values of K_1 can be evaluated. This treatment ignores the charge-transfer complexation of the sterically hindered acceptor ($LuNO^+$).

Associative Equilibria of 2,6-Lutidine and Nitrosonium by Steady-state Voltammetry.—The solution of 10 mmol dm^{-3} NO^+ BF_4^- in acetonitrile containing 0.1 mol dm^{-3} TBAH showed $E_{\frac{1}{2}} = 1.28$ V *vs.* SCE (with traces of NO in evidence) at an ultramicroelectrode (for details, see Bockman, *et al.*).[18] When an aliquot of 2,6-lutidine (Lu, 2 mmol dm^{-3}) was added, the limiting current of NO^+ decreased and a new cathodic wave for $LuNO^+$ appeared at 0.63 V. Upon the incremental addition of Lu, the NO^+ current decreased and the $LuNO^+$ current increased. Both reached steady-state (limiting) levels which remained unchanged upon the further addition of Lu. For the limiting current of NO^+, the associative equilibrium is given as $K_2 = ([NO^+]_0 - [NO^+])/\{[NO^+]([Lu]_0 - [NO^+]_0 + [NO])\}$.

Thermal Activation of Aromatic EDA Complexes with the N-Nitrosopyridinium Acceptor.—Durene. When an equimolar solution of durene and $PyNO^+$ $SbCl_6^-$ in acetonitrile was stirred in the dark, a pale yellow solid separated slowly. Isolation of the pale yellow solid, followed by careful attempts at recrystallization invariably led to decomposition, as indicated by new resonances in the ^1H NMR spectrum at δ 5.77 and 4.61 for *N*-(trimethylbenzyl)pyridinium and benzyl alcohol, respectively. However, the same mixture upon standing in the dark (with no stirring) afforded crystals of **IIa**. $\delta_H(CD_3CN)$ 1.61 (d, 6 H, $J = 1.4$ Hz), 2.17 (s, 6 H), 6.10 (q, 2 H, $J = 1.4$ Hz), 8.11 (t, 4 H, $J = 6.7$ Hz), 8.59 (t, 2 H, $J = 7.6$ Hz) and 8.74 (d, 4 H, $J = 6.0$ Hz); $\delta[(CD_3)_2SO]$ 1.62 (s, 6 H), 2.26 (s, 6 H), 6.28 (s, 2 H), 8.24 (t, 4 H), 8.72 (t, 2 H) and 9.06 (d, 4 H). The *ipso* adduct **IIa** obtained by this procedure was suitable for X-ray crystallography (*vide infra*).

The EDA complex of durene and NO^+ BF_4^- was prepared in acetonitrile and an equimolar amount of pyridine was added at −40 °C. The ^1H NMR spectrum of the dark red solution showed the resonances of durene at δ 2.14, 6.86 and *N*-nitrosopyridinium at δ 8.04, 8.55 and 9.02. When the solution was allowed to warm to room temperature, the colour bleached slowly over the course of a day; ^1H NMR analysis indicated the concomitant disappearance of DUR and $PyNO^+$, together

with the simultaneous appearance of the diagnostic resonances of **IIa** at δ 6.10 (q), 1.62 (d) and 2.06 (s) and those of the isomeric **IIb** 6.10 (q), 1.53 (d) and 2.06 (s). Additional small peaks at δ 1.78, 2.19, 2.23 and 2.30 were assigned to minor products.

1,4-Dimethylnaphthalene. To a solution of $PyNO^+$ $SbCl_6^-$ in acetonitrile at −40 °C was added 1,4-dimethylnaphthalene. The resultant red-brown solution of the EDA complex was allowed to warm to room temperature in the dark. The ^1H NMR analysis of the reaction mixture immediately showed the resonances of the reactants: DMN [δ 7.21 (s), 2.61 (s)] and $PyNO^+$ at δ 8.04, 8.55 and 9.02. After 5 h, DMN was absent, and new resonances at δ 2.44 (s) and 2.25 (s) appeared together with minor peaks at δ 2.10, 2.30, 2.37 and 2.72 in the methyl region. These new resonances were unchanged when the reaction mixture was allowed to stand in the dark for 2 days. In a (dark) control experiment, a solution of DMN and NO^+ BF_4^- without pyridine was unchanged for comparable periods, and after aqueous work-up yielded DMN in essentially quantitative yields. The *ipso* adducts **Ia, b** were isolated by removal of the solvent *in vacuo*. The brown residue was washed with dichloromethane and then dissolved in acetonitrile. Addition of diethyl ether yielded a yellow solid which was recrystallized from a mixture of acetonitrile and dichloromethane. **Ia**: $\delta_H(CD_3CN)$ 2.43 (s, 6 H), 6.49 (s, 2 H), 7.32 (m, 2 H), 7.53 (m, 2 H), 8.09 (t, 2 H, J = 7.0 Hz), 8.58 (t, 2 H, J = 7.6 Hz), 8.80 (d, 2 H, J = 6.1 Hz); $\delta_C(CD_3CN)$ 29.2, 71.5, 128.9, 129.9, 132.5, 132.7, 135.7, 143.8 and 148.3. To the mother liquor, additional diethyl ether was added and the mixture cooled to −20 °C to yield additional amounts of yellow solid. Recrystallization afforded the *ipso* adduct **Ib**, $\delta_H(CD_3CN)$ 2.26 (s, 6 H), 6.49 (s, 2 H), 7.01 (m, 2 H), 7.45 (m, 2 H), 8.16 (t, 4 H, J = 7.0 Hz), 8.65 (t, 2 H, J = 7.7 Hz), 8.93 (d, 4 H, J = 6.0 Hz); $\delta_C(CD_3CN)$ 29.1, 71.5, 127.8, 129.8, 132.0, 132.3, 136.0, 144.5 and 148.3.

The EDA complex of 1,4-dimethylnaphthalene with $PyNO^+$ (prepared *in situ* from NO^+ BF_4^- and pyridine) was prepared at −40 °C by a procedure similar to that described above. When the red-brown solution was allowed to warm in the dark to room temperature, it bleached within an hour, to afford a pale yellow solution the ^1H NMR spectrum of which was virtually identical with that obtained from $PyNO^+$ $SbCl_6^-$.

Hexamethylbenzene. The EDA complex of hexamethylbenzene and $PyNO^+$ BF_4^- was prepared at −40 °C. When the dark solution was allowed to warm in the dark to room temperature the colour lightened considerably, and new resonances appeared in the ^1H NMR spectrum at δ 1.40 and 1.49. These new resonances disappeared completely with those of hexamethylbenzene after a day. The final ^1H NMR spectrum showed resonances at δ 2.19, 2.26, 2.30 and 5.89 in an intensity ratio 6:6:3:2, and it was assigned to *N*-(pentamethylbenzyl)pyridinium cation by analogy with the ^1H NMR spectrum of *N*-(pentamethylbenzyl)-4-cyanopyridinium cation.

Photochemical Activation of Aromatic EDA Complexes with the N-*Nitrosopyridinium Acceptor.*—The charge-transfer photochemical experiments were carried out as described previously.[23] In each case the appropriate cut-off filter was selected as listed in Table 3 to allow specific excitation of the charge-transfer absorption band.

Durene. The EDA complex of durene and $PyNO^+$ $SbCl_6^-$ was irradiated at 0 °C with λ_{exc} > 500 nm. Separation of the *ipso* adduct **IIa** occurred spontaneously and was shown to be identical with that isolated and characterized from the thermal reaction. On the other hand, the irradiation of the durene EDA complex with $PyNO^+$ BF_4^- prepared *in situ* led to a mixture of the *ipso* adducts **IIa, b**. ^1H NMR analysis indicated the distribution of the *cis*/*trans* isomers to be the same as that produced in the dark thermal process.

1,4-Dimethylnaphthalene. The red-brown solution of the EDA complex of 1,4-dimethylnaphthalene and $PyNO^+$ $SbCl_6^-$ was irradiated at −40 °C with λ_{exc} > 540 nm. When the photolysate was monitored by ^1H NMR spectroscopy, the diagnostic resonances of DMN and $PyNO^+$ decreased monotonically and were replaced by those of the *ipso* adducts **Ia** and **Ib**. The final ^1H NMR spectrum was the same as that of the solution produced thermally.

Toluene and p-*Xylene.* Since the yellow solution of the EDA complex of $PyNO^+$ (from NO^+ BF_4^- and pyridine) and toluene persisted for days in the dark, it was deliberately irradiated at −40 °C with λ_{exc} > 380 nm. ^1H NMR analysis indicated the complete disappearance of toluene, and new (methyl) resonances appeared at δ 2.10, 2.24 and 2.44 (intensity *ca.* 3:1:1), together with one at δ 7.54. These were unchanged when the solution was warmed to room temperature. Similarly, the solution of *p*-xylene and $PyNO^+$ BF_4^- was irradiated at room temperature with λ_{exc} > 380 nm. After 8 h, ^1H NMR analysis indicated that *ca.* 50% of the *p*-xylene had been consumed, and new (methyl) resonances appeared at δ 2.07, 2.13, 2.39 and 2.47 together with ones at δ 7.31 and 7.40 in the aromatic region. The products were not examined further. The appearances of small peaks at δ 6.47, 5.66 and 4.83 suggested that the *ipso* adduct, a benzylpyridinium cation, and benzyl alcohol, respectively, were minor products.

X-Ray Crystallography of the ipso *Adduct* **IIb** *from the Charge-transfer Activation of the Durene EDA Complex with* $PyNO^+$ $SbCl_6^-$.—A clear colourless fragment having approximate dimensions 0.75 × 0.70 × 0.60 mm was carved from a much larger block and mounted in a random orientation on a Nicolet R3m/V automatic diffractometer. Since the compound was temperature sensitive, all handling was done under mineral oil. The sample was rapidly transferred to the goniometer and placed in a stream of dry nitrogen gas at −50 °C. The concurrent monitoring of several crystals left exposed to air at room temperature showed absolutely no visual evidence of damage over a 5 day period. The radiation used was Mo-Kα monochromatized by a highly ordered graphite crystal. Final cell constants, as well as other information pertinent to data collection and refinement were: space group, $P2_1/c$ (monoclinic); cell constants, a = 8.412(3) Å, b = 14.022(4) Å, c = 14.026(6) Å, β = 100.07(3)°, V = 1629 Å^3; molecular formula, $C_{20}H_{24}N_2{}^{++}2SbCl_6^-$; formula weight, 961.36; formula units per cell, Z = 2; density, ρ = 1.96 g cm^{-3}; absorption coefficient, μ = 26.8 cm^{-1}; temperature, T = −50 °C; radiation (Mo-Kα), λ = 0.710 73 Å; collection range, $4 \leqslant 2\theta \leqslant 50°$; scan width, $\Delta\theta = 1.20 + (K\alpha_2 - K\alpha_1)°$; scan speed range, 1.5 to 15.0° min^{-1}; total data collected, 2871; independent data, $I > 3\sigma(I)$, 2746; total variables, 174; $R = \Sigma||F_o| - |F_c||/\Sigma|F_o|$, 0.020; $R_w = [\Sigma w(|F_o| - |F_c|)^2/\Sigma w|F_o|^2]^{\frac{1}{2}}$, 0.022; weights, $w = \sigma(F)^{-2}$; and extinction coefficient, x = 0.000 50. The Laue symmetry was determined to be $2/m$, and from the systematic absences noted, the space group was shown unambiguously to be $P2_1/c$. Intensities were measured using the omega scan technique, with the scan rate depending on the count obtained in rapid pre-scans of each reflection. Two standard reflections were monitored after every 2 h or every 100 data collected, and these showed no significant change. During data reduction, Lorentz and polarization corrections were applied, as well as an empirical absorption correction based on psi scans of ten reflections having chi values between 70 and 90°. The structure was solved by interpretation of the Patterson map, which revealed the position of the Sb atom in the asymmetric unit, consisting of one-half dication situated about an inversion centre and one anion. The usual sequence of isotropic and

anisotropic refinement was followed, after which all hydrogens were entered in ideal calculated positions and constrained to riding motion, with a single variable isotropic temperature factor for all of them. In the final refinement H3 was allowed to refine independently, and both of the methyl groups were treated as ideal rigid bodies and allowed to rotate freely. Since the classical signs of extinction were noted, an empirical isotropic extinction parameter was also refined. When all shift/esd ratios were less than 0.1, convergence was reached at the agreement factors above. No unusually high correlations were noted between any of the variables in the last cycle of full-matrix least squares refinement, and the final difference density map showed a maximum peak of about 0.5 e $Å^{-3}$. All calculations were made using the Nicolet SHELXTL PLUS (1987) series of crystallographic programs. Tables of final fractional atomic coordinates, bond distances and angles and thermal parameters have been deposited at the Cambridge Crystallographic Data Centre.*

Acknowledgements

We thank J. D. Korp for crystallographic assistance, and the National Science Foundation, the R. A. Welch Foundation, and the Texas Advanced Research Project for financial support.

* For details of the CCDC deposition scheme, see 'Instructions for Authors (1994), *J. Chem. Soc., Perkin Trans. 2*, 1994, issue 1.

References

1 K. Schofield, *Aromatic Nitration*, Cambridge University Press, Cambridge, 1980.
2 D. L. H. Williams, *Nitrosation*, Cambridge University Press, Cambridge, 1988.
3 F. A. Cotton and G. Wilkinson, *Advanced Inorganic Chemistry*, 5th edn., Wiley, New York, 1988, pp. 332–333.
4 J. Jones and J. Jones, *Tetrahedron Lett.*, 1964, 2117.
5 G. A. Olah, J. A. Olah and N. A. Overchuk, *J. Org. Chem.*, 1965, **30**, 3373. Compare also N. N. Makhova, G. A. Karpor, A. N. Mikhailyuk, A. E. Bova, L. I. Khmel'nitskii and S. S. Novikov, *Izv. Akad. Nauk, SSR*, 1978, 226, and references therein.
6 G. A. Olah, S. C. Narang, J. A. Olah, R. L. Pearson and C. A. Cupas, *J. Am. Chem. Soc.*, 1980, **102**, 3507.
7 G. A. Olah, R. Malhotra and S. C. Narang, *Nitration Methods and Mechanisms*, VCH, New York, 1989, pp. 69–70.
8 E. K. Kim, K. Y. Lee and J. K. Kochi, *J. Am. Chem. Soc.*, 1992, **114**, 1756.
9 E. K. Kim, T. M. Bockman and J. K. Kochi, *J. Am. Chem. Soc.*, 1993, **115**, 3091.
10 S. Sankararaman and J. K. Kochi, *J. Chem. Soc., Perkin Trans. 2*, 1991, 1; E. K. Kim, T. M. Bockman and J. K. Kochi, *J. Chem. Soc., Perkin Trans. 2*, 1992, 1879.
11 See D. L. H. Williams in ref. 2, p. 58ff.
12 K. M. Ibne-Rasa, *J. Am. Chem. Soc.*, 1962, **84**, 4962; B. C. Challis and A. J. Lawson, *J. Chem. Soc. B*, 1971, 770.
13 H. Tsubomura and R. S. Mulliken, *J. Am. Chem. Soc.*, 1960, **82**, 5966.
14 H. B. Benesi and J. H. Hildebrand, *J. Am. Chem. Soc.*, 1949, **71**, 2703.
15 W. B. Person, *J. Am. Chem. Soc.*, 1965, **87**, 167.
16 R. S. Mulliken, *J. Am. Chem. Soc.*, 1952, **74**, 811; R. S. Mulliken and W. B. Person, *Molecular Complexes*, Wiley, New York, 1969.
17 K. Y. Lee, D. J. Kuchynka and J. K. Kochi, *Inorg. Chem.*, 1990, **29**, 4196.
18 T. M. Bockman, Z. J. Karpinski, S. Sankararaman and J. K. Kochi, *J. Am. Chem. Soc.*, 1992, **114**, 1970.
19 *cf.* G. Y. Markovits, S. E. Schwartz and L. Newman, *Inorg. Chem.*, 1981, **20**, 445.
20 (*a*) E. K. Kim and J. K. Kochi, *J. Am. Chem. Soc.*, 1991, **113**, 4962; (*b*) W. G. Fateley, H. A. Bent and B. Crawford, Jr., *J. Chem. Phys.*, 1959, **31**, 204.
21 C. J. Schlesener, C. Amatore and J. K. Kochi, *J. Am. Chem. Soc.*, 1984, **106**, 3567.
22 Compare Fig. 8 in E. K. Kim *et al.* in ref. 8.
23 T. M. Bockman, K. Y. Lee and J. K. Kochi, *J. Chem. Soc., Perkin Trans. 2*, 1992, 1581.
24 (*a*) V. D. Parker, *Acc. Chem. Res.*, 1984, **17**, 243; (*b*) O. Hammerich and V. D. Parker, *Adv. Phys. Org. Chem.*, 1984, **20**, 55 and references therein.
25 W. Lau and J. K. Kochi, *J. Am. Chem. Soc.*, 1986, **108**, 6720.
26 Compare D. T. Shang and H. N. Blount, *Electroanal. Chem. Interfac. Electrochem.*, 1974, **54**, 305.
27 C. Reichardt, *Solvent and Solvent Effects in Organic Chemistry*, 2nd edn., VCH, Weinheim, 1988. See also T. Yabe and J. K. Kochi, *J. Am. Chem. Soc.*, 1992, **114**, 4491. Although the nitrosopyridinyl radical may be an intermediate in eqn. (27), it is likely that the electron transfer is irreversible and derives additional driving force from the simultaneous cleavage of the Py–NO bond.[8]
28 R. Taylor, *Electrophilic Aromatic Substitution*, Wiley, New York, 1990, p. 261ff.
29 See R. Taylor in ref. 28, p. 279.
30 In the corresponding electrophilic process, heterolytic scission would regenerate the aromatic donor and (NO^+) or (NO_2^+).
31 G. Brauer, *Handbook of Preparative Inorganic Chemistry*, 2nd edn., vol. 1, Academic, New York, 1963, p. 511.
32 Compare F. Seel and T. Gössl, *Z. Anorg. Allgem. Chem.*, 1950, **263**, 253.

Paper 3/06171J
Received 15*th October* 1993
Accepted 29*th October* 1993